

Investigation on Failure Loads and Failure Modes for Two Parallel Pin-Loaded Holes Made from Unidirectional Glass-Epoxy Nanoclay Laminates

Sajjad Dehghanpour

Faculty of Industrial and Mechanical Engineering,
Qazvin Branch, Islamic Azad University, Qazvin, Iran
E-mail: sajjaddehghanpour@yahoo.com

Keivan Hosseini Safari *

Department of Mechanical Engineering, Central Tehran Branch, Islamic Azad University,
Tehran, Iran

E-mail: keivan.hosseini.safari@gmail.com

*Corresponding author

Farzan Barati, Mohammadmahdi Attar

Department of Mechanical Engineering,
Hamedan Branch, Islamic Azad University, Hamedan, Iran
E-mail: farzanbarati@yahoo.com, d.attar.iauh@gmail.com

Received: 19 January 2020, Revised: 1 March 2020, Accepted: 30 May 2020

Abstract: Purpose of this study is to obtain failure modes and failure loads of two Parallel pin loaded holes in unidirectional glass fibre/epoxy by adding nanoclay in the absence of nanoclay composite laminates using finite element analysis; the results are validated through experiment. The geometrical parameters studies in this survey include the distance between the diameter of the hole (e/d) and the free edge of specimen, the distance between two holes-to-hole diameter (M/d). The samples were exposed to constant speed tensile loading. The results showed that by adding nanoclay, failure load increases and failure modes varies from shear out to bearing failure. Furthermore, increasing distance from the free edge of the pin centre's increases load bearing capacity of two type of composite materials and changes the failure mode from shear to the bear, it increases and decreases the distance from canter's of pin in layers with and without nanoclay particles, respectively and changes failure mode from shear to bear mode. In order to find morphology of specimens and dispersion quality, Scanning Electron Microscope (SEM) was used. For predicting failure load and differentiating failure modes, Tsai-hill failure criteria associated with material property degradation is used. Experimental and FEM results indicate importance of considering the impact of e/d and M/d ratios in the design of two Parallel pin joints. ANSYS was used to carry out numerical simulation and the results denote a good agreement between numerical and experimental results. In this study, by designing an experimental and numerical procedure to estimate the effect of nanoclay, on failure mode and failure load of typical composite material, glass-epoxy, we could illustrate that adding nanoclay brought with it improvement of shear and tensional strength of glass-epoxy about 10 %.

Keywords: ANSYS Software, Failure Behaviour, Finite Element Analysis, Nano-Composite Material, Nanoclay, Parallel Pin-Joints, Polymer Nano Composites,

Reference: Sajjad Dehghanpour, Keivan Hosseini Safari, Farzan Barati, and Mohammadmahdi Attar, "Investigation on Failure Loads and Failure Modes for Two Parallel Pin-Loaded Holes Made from Unidirectional Glass-Epoxy Nanoclay Laminates", Int J of Advanced Design and Manufacturing Technology, Vol. 13/No. 2, 2020, pp. 119–127.

Biographical notes: **Sajjad Dehghanpour** is faculty member at Islamic Azad University, Tuyserkhan Branch and is pursuing his PhD in Mechanical Engineering at Department of Mechanical Engineering, Islamic Azad University, Qazvin Branch, Iran. **Keivan Hosseini Safari** is Assistant Professor at Department of Mechanical Engineering, Central Tehran Branch, Islamic Azad University. He received his PhD in Mechanical engineering at K.N. Toosi University of Iran. **Farzan Barati** received his PhD in Mechanical engineering with emphasis on mechanical behavior of novel alloys in 2012. He is recruited in IAUH university as a faculty member in Mechanical Engineering at 2005, and at 2016 became Associate Professor of Mechanical Engineering. **Mohammadmahdi Attar** is an Associate Professor in Department of Mechanical Engineering, Hamedan Branch, Islamic Azad University. He received PhD from Science and Research Branch, Islamic Azad University in 2015.

1 INTRODUCTION

Nowadays, composite materials are widely used in a variety of industrial structures including aerospace industry. The development of composite materials has recovered properties such as strength, hardness and temperature-dependent behavior. Fiber geometry determines the above properties and properties of the constituent material and their distribution [1-3]. Tolerance of discontinuous phase against force and prevention of improper movement in composite material increase its strength and this can be achieved through reinforcing material with long strands. In order to reinforce fibers, glass fibers are used due to their relatively high strength and relatively low elastic modulus. Some particles are added to resin to enhance some of the properties and improve performance. Adding nanoparticles which have large surface area and the larger bonds between the particles and the matrix to nanocomposites, improve many of its mechanical, thermal and electrical properties.

The impact of amount of nanoclay added to the epoxy resin dog-bone shape samples was studied by Wai Ho et al [4] and the mechanical properties of the composites including tensile and Vickers' hardness tests were also identified. Compared to the nanocomposite samples without nanoparticles, ultimate tensile strength of 5wt% nanoclay composition is higher and its Vickers hardness value is the largest. SEM images show that adding a certain amount of particles makes the samples hard and strong. Influence of processing strategy and nanoclay content on properties of clay-epoxy nanocomposites including tensile, compressive and impact properties have been studied by Gupta et al [5]. To this end, mechanical mixing and shear mixing methods were used to synthesize Nanocomposites. It was observed that by increasing nanoclay content, tensile modulus of both method increases while the compressive modulus does not change. Moreover, the amount of energy absorbed in mechanical mixing is higher. Morphology of nanoclay dispersed in resin and suspended in acetone was studied by Arun et al [6] using Scanning Electron Microscopy (SEM) and Transmission Electron Microscopy (TEM). The results indicate that adding nanoclay increases compressive strength (off-axis test) of the composited reinforced with fiber. Composites are frequently fastened in engineering. One-pin mechanical connections are widely used due to their low cost, simplicity and easier assembly. However, tension distribution on border of the hole of mechanical joints is stronger because they depend on material properties and etc. Furthermore, less force is resisted due to complexity of the stress field near the holes, directions layers and interference of the pin and hole. Influence of ply orientations of $(0^\circ/45^\circ/90^\circ)$, $(0^\circ/45^\circ/0^\circ)$ and $(0^\circ/90^\circ/0^\circ)$ and nano fillers of 1,2,3,4 and 5 wt% on the bearing strength and failure mode of the pin joints was studied by Saini et al [7] both numerically and empirically. They also investigated the distance between diameter of the hole (e/D) and free edge of the specimen and width of the specimen to the diameter of the holes (W/D) ratio. Results demonstrated dependency of

strength of the pin joints on both ply orientations and nano filler wt%. The pin-loaded glass fiber reinforced by polyethylene laminated composites of various dimensions was studied by Babu et al [8] experimentally in ANSYS considering the stress analysis, failure strength and failure mode. The geometrical parameters are selected as (E/D) ratio and (W/D) ration. Failure and reliability of cross-ply $[0/90]_2s$ glass fiber reinforced epoxy composite pinned-joints was analysed by Khashaba et al [9] considering the impact of pin-hole clearance on the properties of composite pinned-joints. They demonstrated that the first-peak and ultimate strength are decreased by 33.1% and 15.3%, respectively and the pin-hole clearance is increased; the ultimate displacement is increased by 10.7% and the apparent joint stiffness is decreased by 27%. Cooper, Hyer and Klang [10] studied the impact of clearance, friction and pin elasticity on the distribution of stress around the edge of holes in a pin-loaded orthotropic plate. In this study, two pin stiffnesses, two clearance levels, two friction levels and two laminates, a $(0^\circ/\pm 45^\circ/90^\circ)$, and a $(02^\circ/\pm 45^\circ)$ were considered. It was observed that the distribution, stress quantity are significantly affected by friction and clearance and load capacity is increased by pin elasticity. Dejong [11] studied distribution of stress around a pin-loaded hole in an elastically orthotropic plate. He loaded the hole without friction only on one part of its edge using an infinitely rigid pin with the same diameter. In order to estimate the stress on the sheet of limited width, numerical results for three laminated fiber reinforced plastic and three (W/D) ratio of the hole were used. Shishesaz et al [12] studied how distribution of stress around a pin joint in a laminated composite is affected by fiber arrangement. Equilibrium equations were written for square and hexagonal fibers based on the crop failure model and it was founded that stress distribution in the square arrangement is less than the hexagonal arrangement. Furthermore, diameter and position of the whole affect the normal and shear stress of the laminate, significantly. The effect of the nanoclay on the bearing strength and failure mode of the pin joints were studied by Singh et al [13] both experimentally and numerically. They considered (E/D) ration and (W/D) ratio as the geometrical parameters and both of them are varied from 1 to 5. The results showed a good agreement between the experimental and numerical results. Tsai-Wu failure criteria and the methods used to predict the failure characteristics and failure mode analysis showed that the strength and failure mode and geometrical parameters were affected by wt% nanoclay. Shishesaz and Attar [14] considered stress distribution in a unidirectional multilayered composite with two serial pin-load holes. They studied the effect of geometrical parameters such as, edge distance to pin diameter ratio (e/d), pins center to center distance, and size of each pin hole on stress distribution. Stress concentration factors and finite element values were compared. The two methods were in good agreement. Strength of single pin joints in glass fiber-reinforced epoxy laminates containing two different nanoparticles, i.e. nanoclay and nanoTiO₂ were

studied and compared by Sekhom et al [15]. Samples of different geometric parameters such as (E/D) ratio, (W/D) ratio were placed under tensile load. The results indicated that adding nanoclay increases the bearing strength of pin joints compared to adding nanoTiO₂. The impact of geometrical and physical parameters on failure modes and failure loads in unidirectional polymeric matrix composites with two serial pin loaded holes was studied by Attar [16]. Results showed that for two pins of small size, bearing is the dominant failure mode and as size of the hole increases, failure modes change to tension and shear. Nanda Kishore et al [17] studied failure modes and failure loads of multi-pin joints in glass-epoxy composite laminates using FEM and experiment. Dehghanpour et al [18] studied the effect the stress concentration factor around a pin-loaded hole in a metallic matrix composite material, analytically and numerically. They derived the equilibrium equation for all fibres and the metallic matrix, the previous Shear-Lag theory had been improved and the extension in the metallic matrix was considered. In the reviewed papers, the effect of the nanoclay additive on the failure force and failure modes of the composite plates has not been investigated and in addition to the effect of this additive, the effect of geometrical parameters will be investigated.

In this study, the effects of (P/D) ratio, (S/D) ratio and (E/D) ratio were considered. They also considered e/d and M/d ratios on failure mode, failure load and bearing strength in laminated glass/epoxy composite plate in which there are two parallel circular holes exposed to traction forces by two parallel pins. This study is mainly focused on the effects of nanoclay on failure of fiber reinforced composites with matrix. SEM imaging was used to investigate morphology of nanoclay. The results showed that morphology of nanoclay distributed in resin affects mechanical properties of the resin. Failure theory is the motivation of this study. Adding nanoclay increases stiffness of the resin, considerably. Behavior of pin loaded composite plates of various sizes has been studied both numerically and experimentally. For the numerical analysis, two-dimensional finite element methods were used in ANSYS. In order to obtain failure load and failure mode of the laminated plates, Tsai-hill criterion is used.

The main purpose of this study is to investigate failure mode and failure load of unidirectional composite material under two parallel pin joints reinforced by nanoclay addition, numerically and experimentally.

2 EXPERIMENTAL STUDY

2.1. Materials and Fabrication

215.5gr epoxy resin 1012 and 27gr hardener were employed to compose a 3-layer unidirectional fiber composite. In order to manufacture the layers of composited with nanoparticles, 7.5gr nanoclay composite which is 3% of its total weights was added to the epoxy resin. “Table 1” represents

mechanical properties of epoxy resin and Fiber glass. For uniform dispersion of nanoclay platelets, an ultrasonic sonicator was used which transmitted a pulse of ultrahigh frequency (20 kHz) to the mixture with an operating power of 25W. The ultrasonic sonicator was set to sonicate for 2min so that the temperature remains constant (the mixture is cooled). As shown in “Fig. 1(a)”, this process was repeated for 30min. It is obvious that there is no bubble and no particles in the mixture. As can be seen in “Fig. 1(b)”, gel-time retarder was added to the mixture and stirred well. At first, 50*50 fiber glass layers of orientation [03] were made and placed on a mold. The top of fiber layer is coated with about 1/3 of the composition and then, the same fiber layer was put over it. For the resin to be distributed uniformly in the fiber layer and the excess resin to be extruded, a roller was used. The process is repeated by pouring resin (same volume as above) on this fiber layer and placing another dry fiber layer on it until three fiber layers have been laid up, as shown in “Fig. 1(c)”. According to the manufacturer datasheet, at last, the epoxy resin was cured at 100c° and room temperature for three hours and one week. Then, the measured laminated composite was 2 mm thick. In order to make the specimens ready, the laminate plate was cut into given dimensions using a CO₂ CNC machine, as shown in “Fig. 1(d)”.

Table 1 The mechanical properties of fiber and epoxy resin

Properties	Matrix	E-glass fiber
Density (kg/m ³)	1217.9	2491.2
Longitudinal tensile strength (GPa)	0.075	2.658
Longitudinal shear modulus (GPa)	1.0	28.9
Longitudinal passion's ratio	0.35	0.224
Transverse passion's ratio	0.35	0.224
Longitudinal modulus (GPa)	2.7	63
Transverse modulus (GPa)	2.7	63

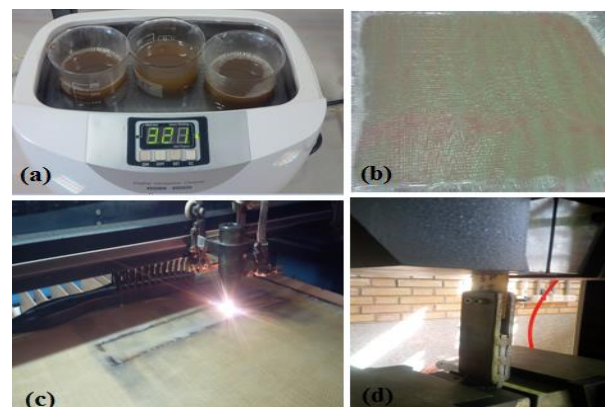


Fig. 1 Making the 3-layer composite: (a): ultrasonic bath; (b): laminate composite; (c): cutting the samples using CO₂ CNC machine, and (d): Tensile testing of specimen.

In order to obtain tensile and compressive performance of laminate, ASTM D3039/ D3039M-14 and D6641/ D6641M [19-20] were used. 80*40 mm samples, 250*25 tensile test samples and two Parallel holes with 5 mm diameter were used.

The process above was used to make another laminate without nanoparticles. Figure 2 shows the samples. 40 samples were used, but to increase accuracy, the process was repeated 3 times. Fixture and position of pins with different (e/d) and (M/d) ratios are shown in "Fig. 3". Diameter of the holes, width and length of the specimen were assumed to be constant.



Fig. 2 Samples from laminate plate with different geometrical parameters.

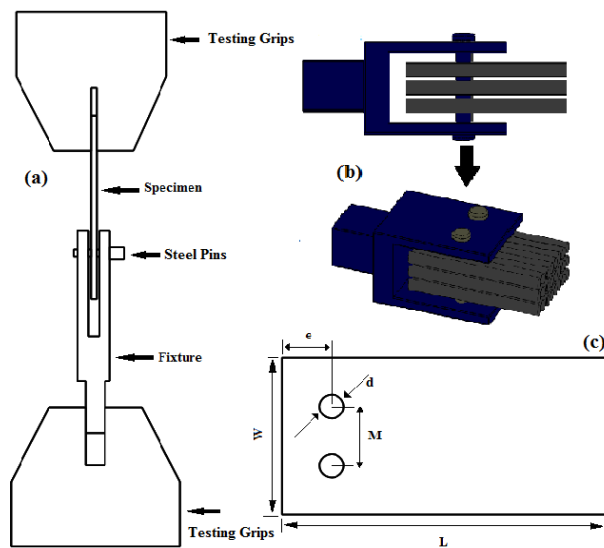


Fig. 3 View of: (a): Self adjustment mechanism, (b): fixture and plate, and (c): geometrical parameters of specimen.

2.2. Testing

In order to perform static (quasi) tension tests, a self-adjustment mechanism as shown in "Fig. 1 (d)", is used. All static tests were performed by SANTAM tensile testing machine with loading capacity of 600 KN using displacement control with 10mm/min cross head speed. It

should be noted that conditions of all tests are the same and SANTAM is used to plot the load versus displacement for every single specimen. The test fixture is designed for all experiments.

3 FINITE ELEMENT SIMULATIONS

This study obtains failure modes and failure loads of glass-epoxy composite laminated plates with two parallel circular holes through a static progressive failure analysis in ANSYS. Due to symmetry of loading, geometry and material composite plate was modelled as a half model. There is no displacement in the symmetry surface along y axis. A two-dimensional, 8-node finite element model (PLANE82) has been used. Plane stress thickness and properties of the orthotropic material of each layer corresponding to the element coordinate directions are the input data. In order to consider the damage, Tsai-hill failure criteria including fiber compression failure, fiber tensile failure, matrix compression failure and matrix tensile failure were used. The nodes behind two pins were fixed in loading direction and perpendicular direction to loading axis. Adaptive refine mesh was used near the holes to improve accuracy. The obtained results indicate that there is a good agreement between numerical and experimental results, but with a slight difference caused by making a large number of specimen manually. Geometry and boundary conditions of the specified model are shown in "Fig. 4".

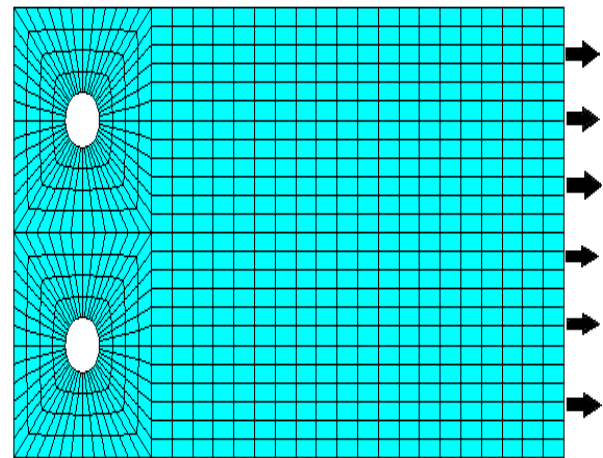


Fig. 4 The geometry and boundary condition of specified model.

4 RESULTS

In this study, failure modes and failure loads of composite specimen which have two pin holes at different positions and dimensions subject to traction force are studied both numerically and experimentally. In order to calculate

failure modes and failure loads of each specimen, three tests were applied. Figures 8 and 9 show the recorded and the plotted load–pin displacement data. In order to predict Maximum carried load and failure modes of the samples in the presence and absence of nanoparticles, Tsai-hill criteria was used as given in “Table 2”. The plastic strain in the matrix (resin) is small and the elastic– plastic modulus of the matrix (resin) with nanoclay is higher than that of the clear resin matrix. By adding nanoclay, initial elastic modulus of resin increases and increasing nanoclay loading results in further improvement. Figure 5 shows the stress-strain curves of the tensile testing of composites in the presence and absence of nanoclay which shows a tensile modulus of 3900 MPa and 2500 MPa in the presence and absence of nanoclay, respectively. Since curvature of the graphs is negligible, the fracture strength is presented as the

tensile strength. As nanoclay content increases, the tensile modulus also increases.

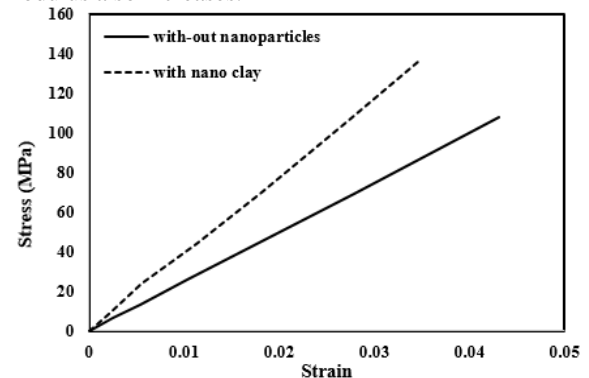


Fig. 5 The tensile stress-strain curves in the presence and absence of nanoclay particles.

Table 2 Failure modes and loads of the composite plate (bearing mode (B), shear-out mode (S), and net-tension mode (N))

	M/D	In the presence of nano-particle					In the absence of nano-particle				
		Experimental			Tsai-hill criterion		Experimental			Tsai-hill criterion	
		Failure load (KN)	Failure Displacement (mm)	Failure Modes	Failure load (KN)	Failure Modes	Failure load (kN)	Failure displacement (mm)	Failure Modes	Failure load (kN)	Failure Modes
e/d=1	2	0.245±0.03	0.3±0.01	S	0.23	S	0.31±0.03	0.345±0.01	S	0.34	S
	3	0.383±0.04	0.7±0.03	S	0.4	S	0.53±0.03	0.604±0.02	S	0.58	S
	4	0.454±0.07	0.6±0.02	S	0.42	S	0.61±0.02	0.537±0.03	S	0.56	S
	5	0.613±0.02	0.9±0.04	S	0.57	S	0.55±0.03	0.822±0.02	S	0.54	S
e/d=2	2	1.36±0.03	0.8±0.05	B/S	1.46	B/S	1.14±0.01	0.86±0.05	B/S	1.19	S
	3	1.34±0.02	1±0.06	B	1.52	B/S	1.15±0.09	1.02±0.02	B/S	1.32	S
	4	1.38±0.06	0.9±0.02	B	1.63	B	0.96±0.08	1.46±0.04	B/S	1.22	S
	5	1.413±0.02	1.2±0.01	B	1.43	B	0.59±0.09	0.38±0.01	B	0.89	S
e/d=3	2	1.3±0.05	1.1±0.01	B	1.51	B	1.08±0.05	0.97±0.08	B	1.13	B/S
	3	1.181±0.04	0.5±0.05	B	0.97	B	1.58±0.08	1.134±0.04	B	1.47	B/S
	4	1.34±0.04	0.7±0.02	B	1.5	B	1.18±0.07	1.14±0.05	B	1.34	B/S
	5	1.565±0.05	1.4±0.04	B	1.7	B	1.09±0.07	1.21±0.03	B	1.25	B/N
e/d=4	2	1.59±0.02	1.1±0.02	B	1.4	B	1.27±0.01	1.03±0.04	B	1.19	B/N
	3	1.732±0.03	1±0.06	B	1.8	B	1.39±0.04	0.877±0.06	B	1.45	B
	4	1.721±0.03	1±0.04	B	1.8	B	1.31±0.06	1.004±0.03	B	1.38	B
	5	1.6360.04	1.2±0.05	B	1.84	B	1.00±0.02	5.72±0.07	B	1.25	B/N
e/d=5	2	1.32±0.02	0.9±0.07	B	1.1	B	1.35±0.03	1.2±0.02	B	1.05	B/N
	3	1.58±0.01	1±0.05	B	1.7	B/N	1.03±0.01	0.788±0.06	B	1.67	B
	4	1.045±0.05	0.7±0.04	B/N	1.2	B/N	1.33±0.04	0.71±0.05	B	1.42	B/N
	5	1.86±0.06	2±0.01	B/N	1.95	B/N	0.61±0.03	1.186±0.04	B	1.28	B/N

Failure regions determine the failure modes. “Table 2” represents the effect of e/d and M/d on failure strength. The bearing strength values significantly depend on e/d ratio as represented in “Figs. 8 and 9”.

As can be seen in “Table 2”, by increasing e/d ratio, the bearing strength of specimen with M/d=2 and M/d=4 ratios and in specimens containing nanoclay particles with M/d=3, increases. Both types of specimen with e/d=1 are

the weakest and the simple specimen with e/d=3 or e/d=4 is the strongest and the specimen with nanoclay is strongest with e/d=4. For e/d=2, bearing strength of all specimen are almost close. By increasing M/d, the bearing strength also increases in the specimen with nanoclay. By adding nanoclay to specimen with e/d=1 except the one with M/d=5, ultimate forces are reduced by 21%, 28% and 26%, respectively. However, in specimen with M/d=5, by adding

nanoclay, ultimate force increases by 11%. Maximum displacement is observed in a specimen with nanoparticles with $e/d=5$ and $M/d=5$ ratio and in a simple specimen with $e/d=4$ and $M/d=5$. For $e/d=4$ in specimen with nanoparticles, failure displacements are close to each other. In order to produce a fresh fracture surface for SEM imaging, resin samples with nanoclay were fractured in liquid nitrogen atmosphere. Mechanical stirring was used to suspend Nanoclay in acetone in the form received from the manufacturer. In order to study the effect of sonication, sonicated suspension of nanoclay in acetone was also prepared. In order to image nanoclay, the filter paper was deposited with drops of the suspensions and acetone was allowed to evaporate. Gold-palladium (AuPd) was used to coat the surface using a sputtering machine for 3 min in an atmosphere enriched with argon to make the samples conductive. Figure 6 shows the SEM images of the samples after failure. Figures 6(a) and (b) show SEM images for 3 wt% nanoclay-epoxy sample and “Fig. 6(c)” shows the simple sample. The cleavage surface and pure epoxy sample are significantly different. As weight of nanoclay inside the epoxy samples increases, the nanoclay introduced to the epoxy acts like the grid lines of a net. Samples with higher nanoclay content have rougher and smaller fracture pieces.

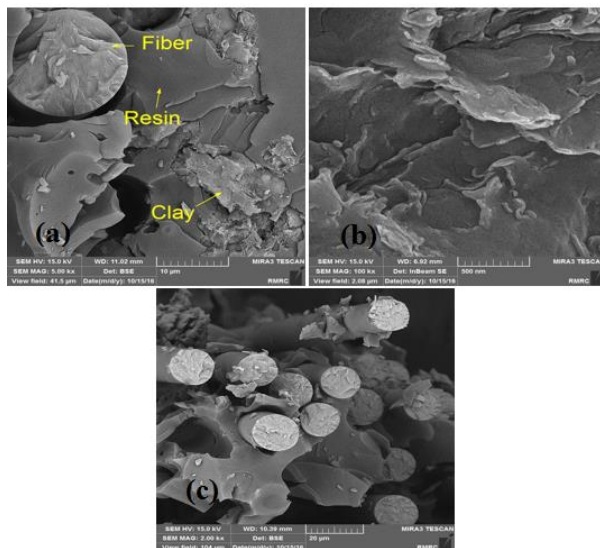


Fig. 6 SEM image of nanoclay dispersed in resin: (a): with resolution $10\mu\text{m}$, (b): with resolution 500nm , and (c): and image of simple specimens with resolution $20\mu\text{m}$.

In order to predict maximum carried load and failure mode in the presence and absence of nanoclay, Tsai-hill criteria were used as shown in “Table 2”. Figure 7 shows results of FEM analysis. It can be seen that there is a good correspondence between numerical and experimental results. However, there is a difference between the experimental and numerical results in terms

of failure modes specially in simple specimen which is due to delamination and matrix cracks. If failure index is equal to or greater than 1, failure occurs. Shear-out mode is obtained for $e/d = 1$ ratios for samples without nanoparticles and with nanoclay. In addition, for specimen with nanoclay, bearing mode is found in the specimens with $e/d = 3$ and 4 for all M/d ratios.

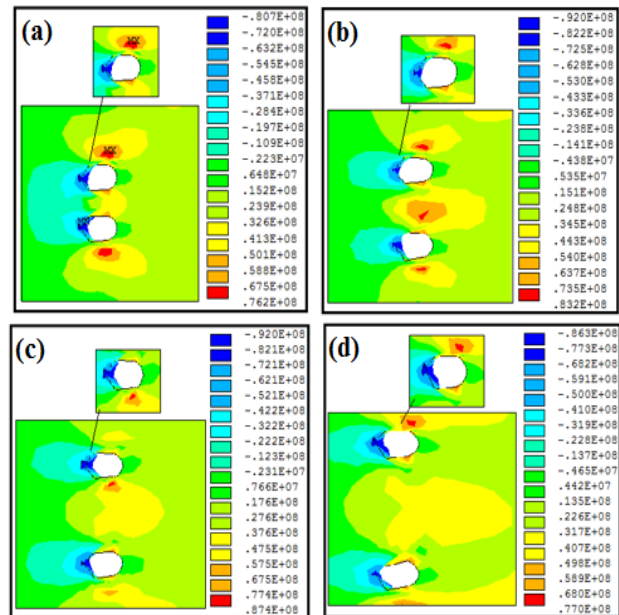


Fig. 7 The stress of specimens (SX) with ratio $e/d=4$ and: (a): $M/d=2$, (b): $M/d=3$, (c): $M/d=4$, and (d): $M/d=5$.

5 DISCUSSION

Upon loading the laminated composite plates to final failure, shearing out, bearing and net-tension modes occur for various geometric dimensions. Before decrease of the first load, the load-pin displacement curves are linear. By increasing the pin displacement after the force peak, the load reduces gradually in some specimens which denotes shearing out failure of the specimen as shown in “Fig. 8(a) and Fig. 9(a)”. Other specimens continue to forward loading. After the first decrease, the load remains constant and rises again which is known as bearing mode which is shown in “Fig. 8(c), (d) and (e)” for simple samples and “Fig. 9(c), (d) and (e)” for samples with added nanoclay. In “Fig. 8. (b)”, a mixed mode of shear out and bearing is shown. Up to pin displacement of 1.2mm , the failure mode is bearing and then the load decreases abruptly which is due to fibre fractures between the pin holes. By pushing the pins, the part in front of two pins moves forward. By increasing the pin displacement, the load continues decreasing indicating that after 1.2mm , failure mode changes to shear out.

Figure 9 (e) shows the mixed mode of bearing and net-tension for ratios $M/d=4$ and 5. The load is carried by the joint up to displacement of 1.5mm. After that, by increasing the pin displacement, the load decreases and

drops abruptly. Damage occurs outside the pins. “Table 2” represents the failure modes of the experimental study. It can be seen that by increasing e/d , failure mode changes to bearing.

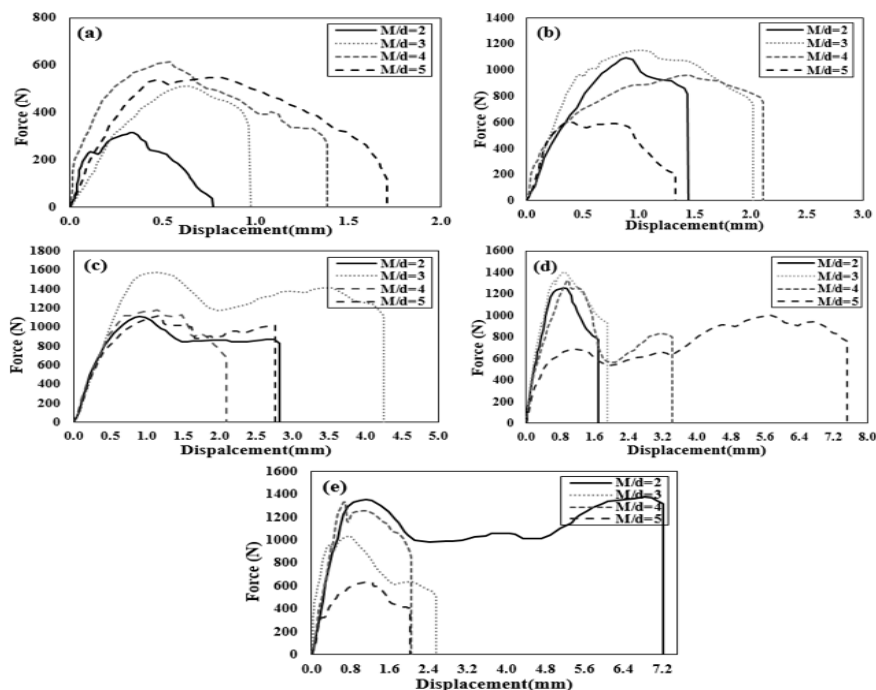


Fig. 8 Load-pin displacement curves for specimen without nanoclay with ratios: (a): $e/d=1$, (b): $e/d=2$, (c): $e/d=3$, and (d): $e/d=4$ (e) $e/d=5$.

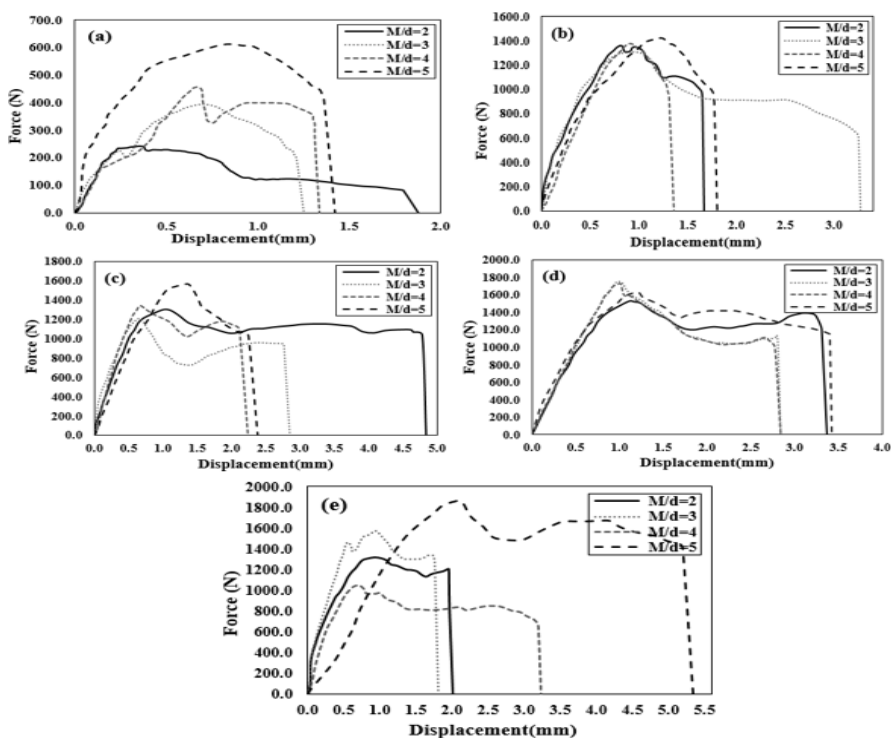


Fig. 9 Load-pin displacement curves of specimens containing clay Nano particles for ratios: (a): $e/d=1$, (b): $e/d=2$, (c): $e/d=3$, (d): $e/d=4$, and (e): $e/d=5$.

Hence, shear out is in direct relationship with e/d ratio. In all specimens, shear out is the failure mode for $e/d=1$. For the specimens with $e/d>2$, failure mode is bearing. The specimens with $e/d=2$ and $M/d=2$, bearing –shear out is the failure mode. Failure mode of the specimens with nanoclay and $e/d=5$ and $M/d=4, 5$ is bearing-net tension. Failure modes of specimens with $e/d=4$ ratio and $M/d=2, 3, 4, 5$ ratios are shown in “Fig. 10”.

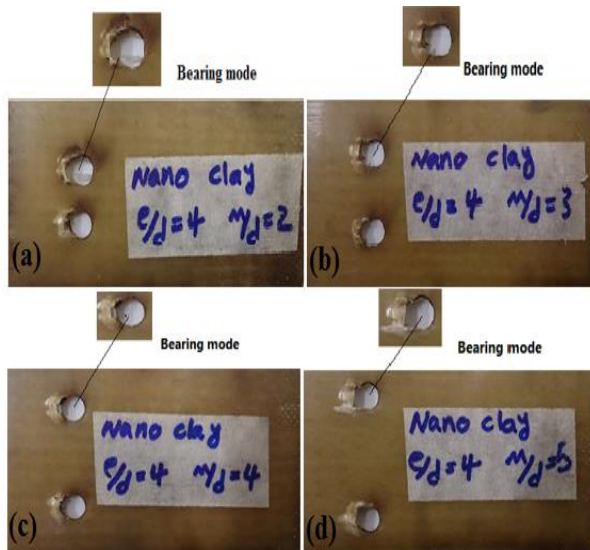


Fig. 10 Failure mode in experimental study for specimens with $e/d=4$ and (a): $M/d=2$, (b): $M/d=3$, (c): $M/d=4$, and (d): $M/d=5$.

6 CONCLUSION

This study obtains failure mode, failure load and bearing strength in glass/epoxy composite plate with two parallel circular holes subject to two pins both numerically and experimentally. In order to evaluate the effects of joint geometry, parametric studies are performed. In order to predict failure load and failure mode in numerical study, Tsai-hill failure criteria were used. The following can be inferred from the experimental and numerical results:

1. By adding nanoclay, initial elastic modulus of resin increases.
2. The shear out failure modes are directly related to e/d ratio. In both samples with $e/d=1$, failure mode is shear out. In the samples with nanoclay and $e/d>1$ and $M/d>2$, failure mode is bearing.
3. The factor which limits obtaining mixed modes is M/d ratio. In simple specimens with $e/d > 2$ ratios, failure mode is mixed, and failure mode of the samples with nanoclay and $e/d=5$ and $M/d > 2$ ratios is bearing-net tension.
4. The bearing strength values significantly depend on e/d ratio. By increasing e/d while M/d is constant, the bearing strength increases. By increasing e/d , bearing strength

increases in simple specimens with $M/d=2$ and $M/d=4$ ratios and in specimens containing nanoclay particles with $M/d=3$.

5. The bearing strength values of the experimental and numerical study are correspondent while their failure modes are different.

REFERENCES

- [1] Agarwal, B. L., Static Strength Prediction of Bolted Joint in Composite Material, AIAA Journal, Vol. 18, No. 11, 1980, pp. 1371-1375.
- [2] Camanho, P.P., Matthews, F. L., Stress Analysis and Strength Prediction of Mechanically Fastened Joints in FRP: a Review, Composites Part A, Vol. 28, No. 6, 1997, pp. 529-547.
- [3] Abd-El-Naby S. F. M., Hollaway, L., The Experimental Behavior of Bolted Joints in Pultruded Glass/Polyester Material, Part 1: Single-bolt joints, Journal of Composite Materials, Vol. 24, No. 7, 1993, pp. 531-538.
- [4] Man-Wai, H., Chun-Ki, L., Kin-tak, L., Dickon, H. L. Ng., and David, H., Mechanical Properties of Epoxy-Based Composites Using Nanoclays, Composite Structures, Vol. 75, 2006, pp. 415-421.
- [5] Gupta, N., Chih Lin, T., and Shapiro, M., Clay-Epoxy Nanocomposites: Processing and Properties, Journal of Mineral, Metal and Materials, Vol. 75, 2007, pp. 61-65.
- [6] Subramaniyan, A. K., Sun, C. T., Enhancing Compressive Strength of Unidirectional Polymeric Composites Using Nanoclay Composites: Part A, Vol. 37, No. 12, 2006, pp. 2257-2268.
- [7] Sekhon, M., Bhunia, H., and Saini, J. S., Effect of Ply Orientation On Strength and Failure Mode of Pin Jointed Unidirectional Glass-Epoxy Nanoclay Laminates, Defence Science Journal, Vol. 65, 2015, pp. 489-499.
- [8] Suresh Babu, V., Tara Sasanka, C., and Ravindra, K., Failure and Stress Analysis of Glass Fiber Reinforced Laminated Composite Pinned Joints, Int J Advanced Design and Manufacturing Technology, Vol. 6, 2013, pp. 13-19.
- [9] Khashaba, U. A., Sebaey, T. A., and Alnefaie, K. A., Failure and Reliability Analysis of Pinned-Joint Composite Laminates: Effects of Pin-Hole Clearance, Journal of Composite Materials, Vol. 47, No.18, 2012, pp. 2287-2298.
- [10] Hyer, M. W., Klang, E. C., and Cooper, D. E., The Effects of Pin Elasticity, Clearance, and Friction On the Stresses in A Pin-Loaded Orthotropic Plate, Journal of Composite Materials, Vol. 21, No. 3, 1987, pp. 190-206.
- [11] Jong, T. D., Stresses Around Pin-Loaded Holes in Elastically Orthotropic or Isotropic Plates, Journal of Composite Materials, Vol. 11, No. 3, 1977, pp. 313-331.
- [12] Shishesaz, M., Attar, M. M., and Robati, H., The Effect of Fiber Arrangement On Stress Concentration Around a Pin in A Laminated Composite Joint, ASME 2010 10th

- Biennial Conference on engineering systems design and Analysis, 2010.
- [13] Singh, M., Saini, J. S., and Bhunia, H., Investigation on Failure Modes for Pin Joints Made from Unidirectional Glass-Epoxy Nanoclay Laminates, *Fatigue & Fracture of Engineering Materials & Structures*, Vol 39, No. 3, 2015, pp. 320-334.
- [14] shishesaz, M., Attar, M. M., Stress Concentration Analysis of Fiber-Reinforced Multilayered Composites with Two Serial Pin-Load Holes, 18th Annual Conference of Mechanical Engineering, 2011.
- [15] Sekhon, M., Saini, J. S., Singla, G., and Bhunia, H., Influence of Nanoparticle Fillers Content On the Bearing Strength Behavior of Glass Fiber-Reinforced Epoxy Composites Pin Joints, *Proceedings of the Institution of Mechanical Engineers Part L: Journal of Materials: Design and Applications*, Vol. 1, 2015.
- [16] Attar, M. M., Barati, F., Ahmadpour, M., and Rezapour, E., Failure Analysis of Unidirectional Polymeric Matrix Composites with Two Serial Pin Loaded-Holes, *Journal of Mechanical Science and Technology*, Vol. 30, No. 6, 2016, pp. 2583-2591.
- [17] Nanda Kishore, A., Malhotra, S. K. and Siva Prasad, N., Failure Analysis of Multi-Pin Joints in Glass Fibre/Epoxy Composite Laminates, *Composite Structures*, Vol. 9, 2009, pp. 266-277.
- [18] Dehghanpour, S., Hosseini Safari, K., Barati, F., and Attar, M. M., Stress Concentration Around of Pin-Loaded Hole in Unidirectional Multi-Layered Metallic Matrix Composite Material, *Journal of Mechanical Science and Technology*, Vol. 33, No. 10, 2019, pp. 4891-4898.
- [19] Karakuzu, R., Taylak, N., Murat Icten, B., and Aktas, M., Effects of Geometric Parameters On Failure Behavior in Laminated Composite Plates with Two Parallel Pin-Loaded Holes, *Journal of Composite Structures*, Vol. 85, 2008, pp. 1-9.
- [20] ASTM D3410 / D3410M – 16, Standard Test Method for Compressive Properties of Polymer Matrix Composite Materials with Unsupported Gage Section by Shear Loading.